JOURNAL OF VIROLOGY, Aug. 2009, p. 7982–7995 Vol. 83, No. 16
0022-538X/09/$08.00+0 doi:10.1128/JVI.00259-09

Deficiency of Niemann-Pick Type C-1 Protein Impairs Release of Human Immunodeficiency Virus Type 1 and Results in Gag Accumulation in Late Endosomal/Lysosomal Compartments▽

Yuyang Tang,[1]# Ihid Carneiro Leao,[2]# Ebony M. Coleman,[1]
Robin Shepard Broughton,[1] and James E. K. Hildreth[1,2]*

Center for AIDS Health Disparities Research, Meharry Medical College, Nashville, Tennessee 37208,[1] and Department of Pharmacology and Molecular Sciences, Johns Hopkins University School of Medicine, Baltimore, Maryland 21205[2]

Received 4 February 2009/Accepted 20 May 2009

Human immunodeficiency virus type 1 (HIV-1) relies on cholesterol-laden lipid raft membrane microdomains for entry into and egress out of susceptible cells. In the present study, we examine the need for intracellular cholesterol trafficking pathways with respect to HIV-1 biogenesis using Niemann-Pick type C-1 (NPC1)-deficient (NPCD) cells, wherein these pathways are severely compromised, causing massive accumulation of cholesterol in late endosomal/lysosomal (LE/L) compartments. We have found that induction of an NPC disease-like phenotype through treatment of various cell types with the commonly used hydrophobic amine drug U18666A resulted in profound suppression of HIV-1 release. Further, NPCD Epstein-Barr virus-transformed B lymphocytes and fibroblasts from patients with NPC disease infected with a CD4-independent strain of HIV-1 or transfected with an HIV-1 proviral clone, respectively, replicated HIV-1 poorly compared to normal cells. Infection of the NPCD fibroblasts with a vesicular stomatitis virus G-pseudotyped strain of HIV-1 produced similar results, suggesting a postentry block to HIV-1 replication in these cells. Examination of these cells using confocal microscopy showed an accumulation and stabilization of Gag in LE/L compartments. Additionally, normal HIV-1 production could be restored in NPCD cells upon expression of a functional NPC1 protein, and overexpression of NPC1 increased HIV-1 release. Taken together, our findings demonstrate that intact intracellular cholesterol trafficking pathways mediated by NPC1 are needed for efficient HIV-1 production.

Human immunodeficiency virus type 1 (HIV-1) is a complex retrovirus highly dependent upon a myriad of cellular mechanisms for successful virus replication. Cholesterol plays a pivotal role throughout the HIV-1 life cycle (23, 40, 41, 64). HIV-1 entry, assembly, and budding processes occur at cholesterol-enriched membrane microdomains known as lipid rafts, and depletion of cellular cholesterol markedly and specifically reduces HIV-1 particle production. Virion-associated cholesterol is required for fusion and subsequent infection of susceptible cells (41), and cholesterol-sequestering drugs, such as β-cyclodextrin, render the virus incompetent for cell entry (4, 25, 57). Therefore, intracellular cholesterol trafficking pathways that allow nascent HIV-1 particles to acquire lipids appear critical for virus replication.

Recent evidence supports a critical role for cholesterol trafficking and homeostasis in viral replication, showing that the HIV-1 accessory protein Nef increases synthesis and transport of cholesterol to both lipid rafts and progeny virions and induces multiple genes involved in cholesterol synthesis (80, 88). More recent studies have revealed that binding of Nef to the ATP-binding cassette transporter A1 (ABCA1) leads to impairment of ABCA1-dependent cholesterol efflux and an accumulation of lipids within the cell (51).

Mammalian cells acquire cholesterol primarily from endocytosed low-density lipoproteins (LDL). The Niemann-Pick type C-1 (NPC1) protein is well known for its role in intracellular trafficking of LDL-derived free unesterified cholesterol. Dysfunctional NPC1 activity leads to development of NPC disease, a rare, autosomal recessive, neurodegenerative disorder characterized by the massive accumulation of cholesterol and glycosphingolipids in late endosomal/lysosomal (LE/L) compartments (61). In normal cells, endocytosed LDLs are delivered to the LE/Ls, where they are hydrolyzed and free cholesterol is released. Homeostasis is achieved when cholesterol is then rapidly transported out of the LE/Ls to the plasma membrane and endoplasmic reticulum (ER) (17, 19, 42, 73, 85), or first to the *trans*-Golgi (TG) network (TGN) and then to the ER (76). In NPC1-deficient (NPCD) cells, the cholesterol does not exit the endocytic pathway, resulting in its accumulation within LE/L structures.

In 95% of NPC patients, the disease is caused by mutations in the NPC1 gene, while the remaining 5% harbor mutations in the NPC2 gene (50, 72, 79). One of the most frequently found and extensively characterized NPC1 mutations is the I1061T mutation (37, 38, 86). This mutation results in misfolding of the NPC1 protein, leading to its degradation and causing an 85% decrease in cellular NPC1 expression (20). Cells with such low levels of functional NPC1 maintain only 38% of normal sphin-

* Corresponding author. Mailing address: Center for AIDS Health Disparities Research, George Hubbard Hospital, Rm. 5035, Meharry Medical College, 1005 DB Todd Blvd., Nashville, TN 37208. Phone: (615) 327-5890. Fax: (615) 327-6929. E-mail: jhildreth@mmc.edu.
# These authors contributed equally to this work.
▽ Published ahead of print on 27 May 2009.

gomyelinase activity and have impaired cholesterol esterification and trafficking.

NPC1 is a large, multispanning protein that resides in the limiting membrane of the LE and binds cholesterol via its N-terminal domain (31). While the complete physiological function of NPC1 is still unclear, NPC1 does share homology with the resistance-nodulation-division family of prokaryotic permeases and may function as a transmembrane efflux pump to transport cargos in LEs (9, 75). Other studies suggest that NPC1 might also function in vesicle-mediated pathways for cargo transportation from LEs to other intracellular sites (21, 33). Recent studies by Infante et al. have propelled forward our understanding of how NPC1 works together with NPC2, also known to bind cholesterol, to support cholesterol efflux from the LE (32). Their findings provide a basis for either of two possible models, with respect to cholesterol trafficking: (i) NPC1 binds cholesterol found within the LE and mediates either direct export or transfer to NPC2 for delivery to a cholesterol efflux transporter, such as ABCA1; or (ii) NPC2 is the first to bind cholesterol and then mediate its delivery to NPC1 for direct export or transfer to ABCA1. These recent findings underscore the highly critical role of these proteins in maintaining intracellular cholesterol homeostasis.

In addition to its role in sterol trafficking, some studies suggest that the NPC pathway may be directly involved in trafficking multiple proteins from LE/L compartments. LEs act as sorting stations to deliver endocytosed molecules to L's for degradation, while at the same time retrieving other classes of proteins and lipids for transport back to nondegradative compartments (3, 14, 15, 28, 63, 69, 78). LE compartments also serve as sorting stations for HIV-1 viral proteins and represent a major site for HIV-1 assembly and budding (7, 12, 16, 22, 24, 57, 59).

The endosomal trafficking defects observed in NPCD cells extend to proteins such as IGF2/MPR, NPC1, and annexin II, all of which utilize the endosomal recycling pathway (42, 74). Electron microscopy studies have shown that within the LEs of NPCD cells these proteins are trapped in the cholesterol-enriched membrane-bound vesicular structures (47). Cholesterol and glycosphingolipid accumulation within NPCD cells appears to disrupt Rab9 GTPase function in LE-to-TGN transport, trapping Rab9-associated proteins, such as vimentin, Tip47, and the mannose-6-phosphate receptor in LEs (18, 83). Overexpression of Rab7 and Rab9 GTPases can reverse the cholesterol accumulation phenotype caused by NPCD (8, 84). These observations suggest that NPC1, directly or indirectly, plays a role in protein export from LEs. It is unknown whether NPC1 is involved in the export of HIV-1 proteins from LEs; however, the Rab9 GTPase-mediated pathway is known to be required for HIV-1 replication (53). This strongly suggests that HIV assembly will be hindered when the NPC pathway is disrupted.

Given the function of NPC1 in mediating intracellular cholesterol trafficking within the LE and given the need of HIV-1 for cholesterol, NPC1 involvement in HIV-1 biogenesis is highly likely. In the present study, using cells treated with U18666A or NPCD cells, we show that impaired NPC1 function results in profound suppression of HIV-1 replication. Further, our findings demonstrate that the NPC1 protein is essential for proper trafficking of the HIV-1 Gag protein during the late stages of assembly and budding. It appears that in NPCD cells, in which cholesterol and cellular proteins accumulate in LE/L compartments, the viral Gag protein fails to traffic properly and accumulates within these compartments, resulting in decreased particle production. Our findings not only reinforce the dependence of HIV-1 on cholesterol homeostasis but also support a role for NPC1 in HIV-1 viral protein trafficking and particle release from infected cells.

MATERIALS AND METHODS

Reagents, plasmids, and antibodies. U18666A (3β-[2-(diethylamino)ethoxy]androst-5-en-17-one, HCl) was purchased from Biomol (Plymouth Meeting, PA). Filipin was supplied by Sigma Chemical Co. (St. Louis, MO). The plasmids used for the pseudovirus production (pNL4-3.Luc.R-E plasmid and pHEF-VSV-G) were generous gifts from Janice Clements (Jonhs Hopkins University, Baltimore, MD). pEGFP was a kind gift from Carolyn Machamer (Johns Hopkins University, Baltimore, MD). pNL4.3 was obtained from Malcolm Martin through the NIH AIDS Reference and Reagent Program. The HIV-1 Gag expression plasmid was kindly provided by Stephen Gould (Johns Hopkins University, Baltimore, MD). The expression construct for human NPC1 was obtained from Origene (Rockville, MD). The mouse NPC1 cDNA construct and Rab9 plasmid were generous gifts from M. P. Scott and Suzanne Pfeffer, respectively (Stanford University, Stanford, CA). This NPC1 construct consists of the mouse NPC1 cDNA inserted into a pEGFP-N3 backbone (Clontech, Palo Alto, CA). Monoclonal antibodies against Gag (GagM1), CD63 (H5C6), and LAMP-2 (H4B4) and a rabbit anti-Gag polyclonal antibody used in the study were generated in our laboratory. Commercially available antibodies against NPC1 (Novus Biologicals), green fluorescent protein (GFP) (Clontech), β-tubulin (Santa Cruz Biotechnology, Inc., Santa Cruz, CA), and actin (Sigma, St. Louis, MO) were used for the immunoblotting experiments. Secondary antibodies (goat anti-mouse Fcγ or heavy- and light-chain specific, fluorescein isothiocyanate [FITC] conjugated, horseradish peroxidase goat anti-rabbit Fcγ specific) were obtained from Jackson ImmunoResearch Laboratories (Westgrove, PA). LysoTracker Red DND-99 was obtained from Invitrogen (Eugene, OR). Pharmaceutical-grade 2OHpβCD (Trappsol; molecular weight of ~1,483 to 1,657) was obtained from CTD, Inc. (Gainesille, FL).

Cells. The reporter cell line LuSIV, derived from the CEMX174 cell line, was produced in our laboratory in collaboration with Janice Clements (67). Jurkat T cells were obtained from the American Type Culture Collection (Rockville, MD) and cultured in complete RPMI (cRPMI) medium with 10% fetal calf serum (FCS). TZM-bl HIV-1 indicator cells, a derivative of HeLa cells and obtained from the NIH AIDS Research and Reference Reagent Program (Germantown, MD), were maintained in Dulbecco modified Eagle medium supplemented with 10% FCS. Epstein-Barr virus (EBV)-transformed B lymphocytes and primary fibroblasts, from the same patient carrying a mutation in the NPC1 protein, and normal fibroblasts (GM03124, GM03123, and GM05659) were obtained from Coriell Repositories (Coriell Institute for Medical Research, Camden, NJ). The EBV-transformed B lymphoblasts were maintained in RPMI 1640 (Gibco-BRL/Life Technologies, Gaithersburg, MD) supplemented with L-glutamine, 10 mM HEPES (pH 7.2), 20% FCS (cRPMI) (HyClone, Logan, UT). EBV-transformed lymphoblasts from healthy donors, established in our laboratory, were maintained under the same culture conditions. Fibroblasts were maintained in Dulbecco modified Eagle medium (Gibco-BRL/Life Technologies, Gaithersburg, MD) supplemented with L-glutamine, 10 mM HEPES (pH 7.2), 10% FCS (cRPMI) (HyClone, Logan, UT). Cell viability was assessed by flow cytometry using 7-amino-actinomycin D (Molecular Probes, Eugene, OR) and by trypan blue exclusion methods.

Viruses. HIV-1 was purified from culture supernatants of infected cells by ultracentrifugation through a sucrose cushion, as previously described (23). Stocks of HIV-1_{MN} were obtained from the NIH AIDS Research and Reference Reagent Program. Purified HIV-1_{BaL} was obtained from ABI (Advanced Biotechnologies, Columbia, MD). CD4-independent HIV strain HxBc2-8X was obtained from James Hoxie (University of Pennsylvania, Philadelphia, PA) (27), and virus stocks were produced in SupT1 cells. Vesicular stomatitis virus (VSV G)-pseudotyped HIV-1 was prepared from 293T cells by transfection with the cloned pNL4.3 plasmid in combination with the VSV G expression vector pHEF-VSVG using Lipofectamine (Invitrogen, Carlsbad, CA) per the manufacturer's instructions. The culture supernatant containing virus particles was harvested 48 h later and either used for infection directly or concentrated by pelleting at 14,000 rpm for 3 h with or without a 20% sucrose cushion (Beckman SW28i); virion pellets were resuspended in phosphate-buffered saline (PBS).

Infections and transfections. LuSIV (2×10^5 cells/0.1 ml), Jurkat (5×10^4 cells/ml), and TZM-bl (2×10^4 cells/0.1 ml) cells were incubated in the presence or absence of various concentrations of U18666A for 24 to 48 h and then infected with various concentrations of HIV-1 (normalized by p24) for 48 h, also in the presence or absence of U18666A at the same concentration as that used in pretreatment. Normal and NPCD lymphoblasts were plated at 2×10^4 cells/0.1 ml and infected overnight with HIV-1_{8x} virus at increasing multiplicities of infection. The following day, the cells were washed to remove residual virus and cultured in fresh media. Normal and NPCD fibroblasts were plated at 2×10^4 cells/ml and infected overnight with 3 μg of VSV G–HIV-1. Cells were then washed to remove residual virus and cultured in fresh media. Normal and NPCD fibroblasts were transfected with full-length proviral DNA clone pNL4.3 or with a human NPC1 construct using the human dermal fibroblast Nucleofector system (Amaxa, Gaithersburg, MD) per the manufacturer's instructions. TZM-bl cells were transfected with pNL4.3, mouse NPC1-pEGFP, Gag, and/or pEGFP plasmids at different molar ratios using Lipofectamine (Invitrogen, Carlsbad, CA) per the manufacturer's instructions. Infection and transfection efficiencies were determined using flow cytometry. Briefly, cells were fixed with 2% paraformaldehyde, permeabilized using 0.1% saponin, and then stained with the mouse KC57-FITC anti-p24 antibody (Beckman Coulter, Inc., Fullerton, CA) or an isotype-matched negative control. Stained cells were analyzed using a Beckman FACSCalibur flow cytometer equipped with Cell Quest software. Viral infection and transfection rates were expressed as percentages of cells staining positively with the anti-p24 antibody.

Cell staining. For cholesterol staining, cells were grown on 35-mm glass-bottom dishes (MatTek Corporation, Ashland, MA) under normal growth conditions and then fixed in 2% paraformaldehyde in PBS for 15 min. The cells were then incubated with filipin at 50 μg/ml in PBS on ice for 30 min. Analysis of filipin staining was performed using a Nikon TE2000 wide-field microscope (Nikon Instruments, Melville, NY). All images were acquired with a plain fluor 60× 1.3-numerical aperture oil immersion objective with a UV fluorescence filter. The digital image acquisition was performed with a Photometrics CoolSNAP HQ2 cooled charge-coupled device camera (Roper Scientific, Tucson, AZ) and Nikon Elements Advanced Research software (Nikon Instruments, Melville, NY). For immunofluorescence studies, cells were grown on acid-washed coverslips or 35-mm glass-bottom dishes to a density of 1 to 5×10^4 cells. The cells were fixed with 2% paraformaldehyde for 20 min and then blocked with 5% normal goat serum and 1% bovine serum in PBS before being permeabilized with 0.1% saponin. Primary antibody anti-Gag (GagM1 or KC57-FITC), anti-LAMP2, or anti-CD63 was incubated with the cells in the blocking solution for 1 h at a final concentration of 10 μg/ml. The cells were then washed two times and incubated with secondary antibodies, FITC- or Texas Red-conjugated goat anti-mouse and Texas Red-conjugated streptavidin (Jackson, Amershan Bioscience, Piscataway, NJ), for an additional hour. For Lysotracker Red staining, cells were incubated with 75 nM LysoTracker Red DND-99 for 1 h at 37°C. The media were refreshed, and the cells were visualized using fluorescence microscopy. The coverslips were mounted onto glass slides using ProLong antifade mounting media (Molecular Probes, Eugene, OR). The slides or glass-bottom dish was examined using a Nikon TE2000 C1 laser scanning confocal microscope (Nikon Instruments, Melville, NY) with a 60× 1.4-numerical aperture oil immersion objective and analyzed using Nikon Elements Advanced Research software.

Virus titer determinations. Three to 10 days postinfection, reverse transcriptase (RT) activity present in the supernatant of infected cell cultures was measured using a commercial kit with a sensitivity of 0.02 mU/ml (Cavidi Tech AB, Uppsala, Sweden). Virus released from infected cells was quantified using a standard enzyme-linked immunosorbent assay (ELISA) developed in our laboratory to measure supernatant levels of the viral p24 antigen (sensitivity 50 to 200 pg/ml) (41). Luciferase assays were performed with infected LuSIV and TZM-bl cells to determine virus replication and titers using a luciferase reporter gene assay system with extended-glow light emission kinetics (Luc-Screen kit; Applied Biosystem, Foster City, CA).

Infectivity assays. Jurkat cells were plated at a density of 2×10^4 cells/0.1 ml and infected overnight with sucrose-pelleted virus generated from infected, normal, and NPCD lymphoblasts. The cells were then washed and maintained under normal culture conditions. Virus present in the supernatant was measured at 15 days postinfection using the p24 ELISA described above. To measure cell-associated transmission, 2×10^4 normal and NPCD lymphoblasts, infected with HIV for either 20 or 39 days (and with comparable levels of intracellular Gag staining), were cocultured with 2×10^4 Jurkat cells for 3 days. The amount of Gag in the supernatant was then quantified by a p24 ELISA.

Quantitative analysis of HIV-1 ERT products. Normal and NPCD lymphoblasts (2×10^6) were infected with HIV-1_{8x} virus at increasing multiplicities of infection in six-well plates. At 8, 24, and 48 h postinfection, equal aliquots of cells were collected and washed with PBS, and total cellular DNA was isolated from the cells using a DNeasy DNA isolation kit (Qiagen). The primers for detection of early reverse transcription (ERT) have been described elsewhere (34, 39). Real-time PCR assays were performed on iCycler using iQ Sybr green supermix (Bio-Rad). All analyses were performed at least three times, with triplicate samples in each experiment.

Electron microscopy. Normal and NPCD lymphoblasts were either mock infected or infected with HIV-1_{8x} and processed 20 days postinfection for transmission electron microscopy, as described by Hendricks et al. (26). Briefly, cells were fixed with 2.5% glutaraldehyde in 100 mM cacodylate-HCl buffer (pH 7.4), 7.5% sucrose and then subjected to postfixation with 4% glutaraldehyde in 0.1 M cacodylate-HCl buffer for 1 h. The cells were then incubated in diaminobenzidine and postfixed in 0.1 M cacodylate buffer containing 1% reduced OsO4, 1% KFeCN. Cells were dehydrated in graded ethanols and embedded in Epon. The fixed samples were then sectioned in a Reichert ultracut E ultramicrotome. Sections were stained with lead nitrate. Micrographs were taken on a Philips CM 10 transmission electron microscope (Philips Scientific, Mahwah, NJ), and images were processed with Adobe Photoshop (Adobe Systems, Inc., Mountain View, CA).

Sodium dodecyl sulfate-polyacrylamide gel electrophoresis and immunoblotting. Cell lysates were prepared by adding 250 μl of NP-40 lysis buffer (0.05 M Tris, pH 7.5; 0.1 M NaCl, 0.002 M EDTA; 1% NP-40; and one protease inhibitor tablet per 25 ml; Roche catalogue no. 1873580) to the cell monolayer after infection or transfection. After quantifying the total amount of protein present in the cell lysate using a bicinchoninic acid protein assay kit (Pierce-Rockford, IL), equal amounts of protein and gel loading dye were mixed. Samples were heated at 70°C for 10 min and then loaded onto 10% or 4 to 12% sodium dodecyl sulfate-polyacrylamide gel electrophoresis gradient gels (NuPAGE Novex Bis-Tris gels; Invitrogen). Proteins were transferred onto a Hybond-P polyvinylidene difluoride membrane (Amersham Biosciences, NJ) according to standard procedures. The membranes were blocked in 3% membrane blocking agent (Amersham Biosciences, NJ) in PBS with 0.1% Tween and then probed with GagM1 and anti-NPC1 antibodies at a 1:500 dilution. The membranes were then incubated with horseradish peroxidase-conjugated, anti-mouse (1:10,000) or anti-rabbit (1:10,000) immunoglobulin G secondary antibodies (Promega, San Luis Obispo, CA) and developed using enhanced chemiluminescence (Amersham Biosciences, NJ). Bands were visualized using Kodak BioMax MR film. Virus lysates were generated from virions containing supernatant and concentrated by pelleting and resuspending them in NP-40 lysis buffer. Loading volume for viral lysates was normalized based on the cell lysate protein amount.

2OHpβCD treatment. NPCD and normal fibroblasts were infected with VSV G/pNL4.3. Four days later, cells were washed and treated with 3% 2OHpβCD in serum-free medium for 1 h at 37°C, as previously described (41). The cells were then washed, put in fresh serum-free medium, and incubated at 37°C. Supernatant was collected at different time points, and the amount of Gag in the supernatant was measured using a p24 ELISA.

Statistical analysis. All experiments were performed two to five times, and representative experiments are shown. The Student *t* test was used to determine the statistical significance of the differences.

RESULTS

U18666A treatment of cells causes cholesterol accumulation and inhibits HIV-1 production. To examine the degree to which productive HIV-1 infection relies on intracellular cholesterol trafficking pathways, HIV-1_{MN}-infected LuSIV cells were treated with U18666A. A class 2 amphiphilic hydrophobic amine, U18666A interferes with intracellular cholesterol transport through inhibition of desmosterol reductase, the enzyme responsible for reducing desmosterol to cholesterol in the cholesterol biosynthetic pathway (6, 62). It also inhibits an additional component involved in cholesterol synthesis, oxidosqualene cyclase (13, 70). This well-studied compound has been shown to induce an NPC disease-like phenotype, with respect to cholesterol accumulation in normal cells (55, 60, 66).

Infected LuSIV cells were incubated with increasing concentrations of U18666A for 48 h and then stained with filipin to examine cholesterol distribution using fluorescent microscopy

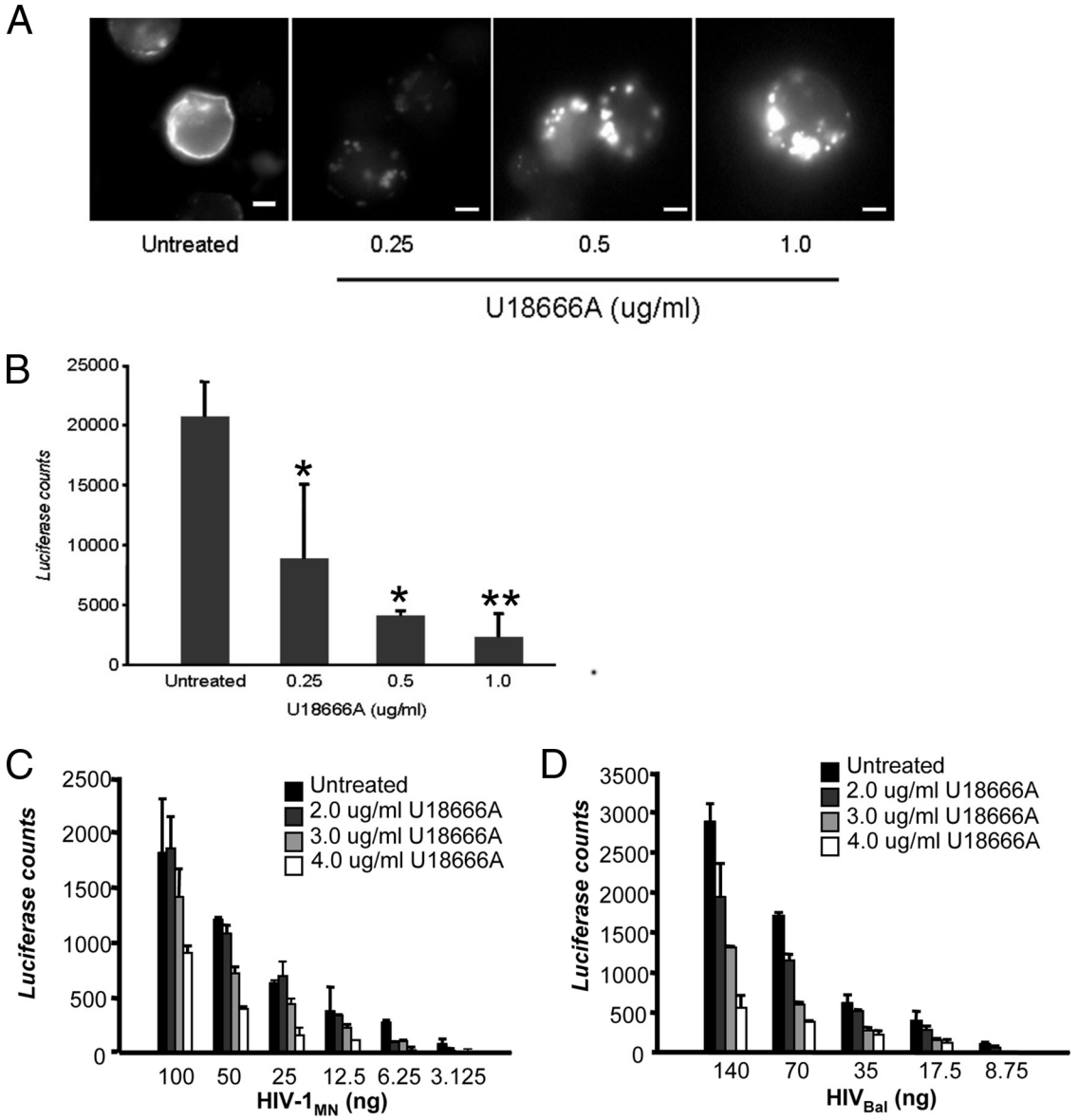

FIG. 1. U18666A treatment of cells causes cholesterol accumulation and inhibits HIV-1 production. (A) LuSIV cells were untreated or treated with U18666A at the concentrations indicated. The cells were stained with filipin and examined by fluorescence microscopy to determine cholesterol phenotypic changes. Scale bars represent 20 μm. (B) LuSIV cells were untreated or treated with U18666A at the concentrations indicated for 24 h and then exposed to 10 ng of HIV-1_{MN} for 48 h in the presence of the compound at the pretreatment concentration. Virus production was measured using a luciferase assay. The data shown represent the mean ± standard deviation from three independent experiments. *, $P < 0.05$; **, $P < 0.001$, compared to cells without U18666A treatment. TZM-bl cells were untreated or treated with U18666A at the indicated concentrations and exposed to X4-tropic HIV-1_{MN} (3.125 to 100 ng p24/2 × 10^4 cells) (C) or R5-tropic HIV-1_{BaL} (8.75 to 140 ng p24/2 × 10^4 cells) (D) for 48 h in the presence of the compound at the pretreatment concentration. Virus replication was measured using a luciferase assay. The data shown represent the mean ± standard deviation from three independent experiments.

(Fig. 1A). There was no toxicity associated with U18666A treatment of the infected cells, as determined by trypan blue exclusion and 7-amino-actinomycin D staining (data not shown). Induction of the NPC disease phenotype was observed with the U18666A-treated cells in a dose-dependent fashion without the need for prior cholesterol depletion. Cholesterol redistribution was evident at the lower concentration of 0.25 μg/ml (less than 0.5 μM), while at the higher U18666A concentration, the NPC disease phenotype was even more pronounced.

LuSIV cells, derived from the CEMx174 hybrid T-cell/B-cell line, contain a luciferase reporter gene and support replication of both HIV-1 and simian immunodeficiency virus isolates (67). To test the effects of the U18666A compound, with respect to HIV-1 infection, virus replication in the HIV-1_{MN}-infected LuSIV cells in the presence or absence of U18666A was measured using a luciferase assay (Fig. 1B). Upon treatment of infected cells with U18666A, there was a 50 to 90% reduction in virus replication that appeared to be dose dependent, such that a higher concentration of U18666A correlated

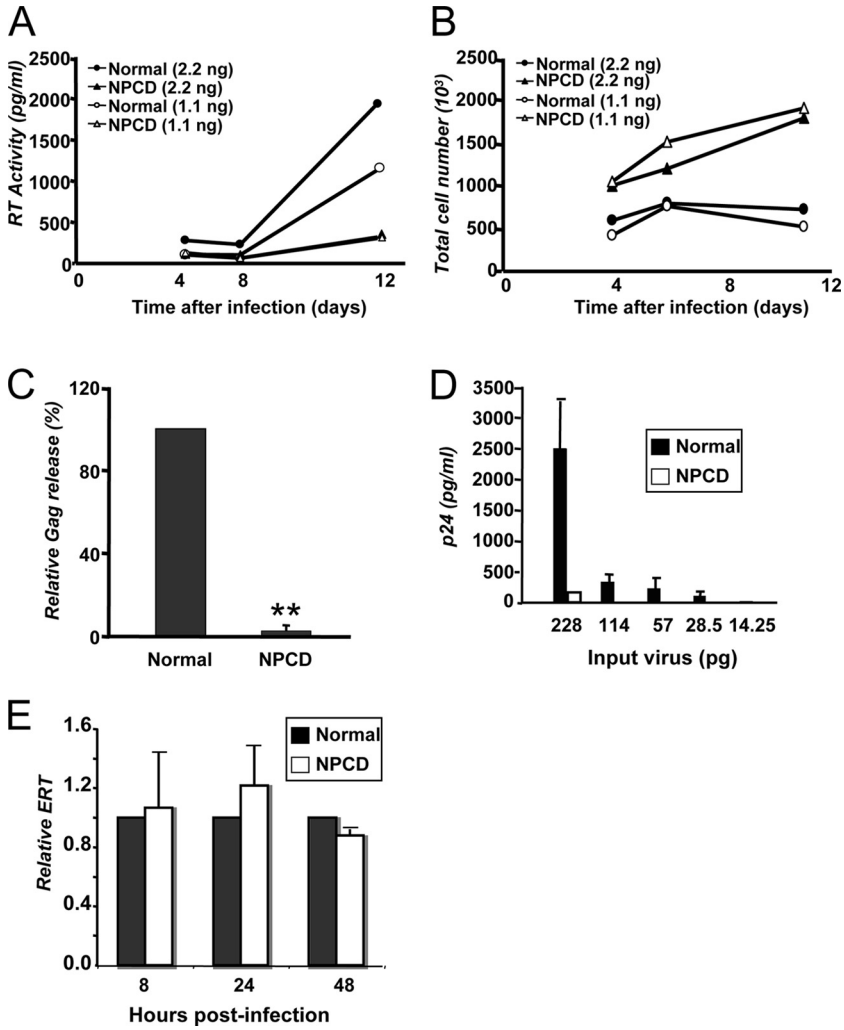

FIG. 2. HIV-1 replication is suppressed in NPCD lymphoblasts. (A) Normal lymphoblasts (circles) and NPCD lymphoblasts (triangles) were infected with either 2.2 ng (filled) or 1.1 ng (open) of HIV_{8X}. At 4, 6, and 11 days postinfection, RT activity in the supernatant was measured. The results shown are the means of five independent experiments. (B) Total cell number was determined for each of the infected cell populations represented in panel A at the same time points after infection. The results shown are the mean of five independent experiments. (C) Normal and NPCD lymphoblasts were infected with 2.2 ng of HIV_{8X}. At 30 days postinfection, the amount of Gag released into the supernatant was measured by a standard p24 ELISA. The relative amounts of Gag are the percentage of normal cells infected with the same amount of virus (arbitrarily set as 100%). The results shown represent the mean ± standard deviation from three independent experiments. **, $P < 0.001$, compared to infected normal lymphoblasts. (D) Normal (black bars) and NPCD (white bars) lymphoblasts were infected with 2.2 ng of HIV_{8X}. At 15 days postinfection, virus-containing supernatants were collected and purified. Virus produced from each cell type was normalized by p24, and comparable amounts were used to infect Jurkat cells. The amount of Gag released by the Jurkat cells into the supernatant was measured by a standard p24 ELISA. The results shown represent the mean ± SD from three independent experiments. (E) Relative levels of HIV-1ERT were quantified by real-time PCR in HIV_{8X}-infected normal (black bars) and NPCD (white bars) lymphoblast cells at the indicated time points. The relative ERT is normalized to normal cells (arbitrarily set as 1). The results shown represent the mean ± standard deviation from three independent experiments.

with lower virus yield. In U18666A-treated TZM-bl cells infected with either an X4- or R5-tropic virus, there was a 70 to 75% reduction in viral replication (Fig. 1C and D). Similar findings were observed with drug-treated $HIV\text{-}1_{MN}$-infected Jurkat cells (60 to 70% decrease in virus replication; data not shown). Taken together, these findings demonstrate that by disrupting intracellular cholesterol transport, U18666A is capable of inducing an NPC disease-like phenotype in HIV-1-infected cells and inhibits viral replication.

HIV-1 infection of NPCD cells results in low levels of virus production. To further investigate the link between HIV-1 infection and intracellular cholesterol pathways, we decided to take advantage of NPCD cells. As these pathways are severely compromised in NPC disease, these cells serve as an excellent tool to study the precise level at which cholesterol is impacting the HIV-1 replication cycle. To that end, we obtained EBV-immortalized primary B lymphocytes derived from a healthy donor and from a patient with NPC disease caused by the I1061T mutation. While they expressed similar levels of CXCR4, as determined by flow cytometry (data not shown), both the normal and NPCD lymphoblasts were found to be CD4 negative.

To overcome this limitation, a CD4-independent strain of HIV-1 (HIV_{8X}) was used to infect these cells (Fig. 2). A vari-

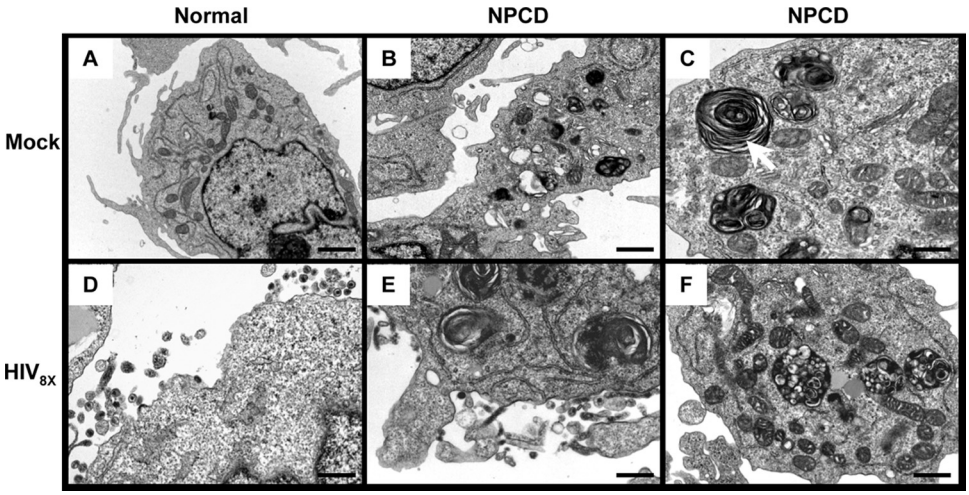

FIG. 3. Viral particle assembly and budding are impaired in HIV-1-infected NPCD lymphoblasts. Normal (A and D) and NPCD lymphoblasts (B, C, E, and F) were uninfected (A, B, and C) or infected (D, E, and F) with 2.2 ng of HIV_{8X}. At 20 days postinfection, the cells were processed for and examined by electron microscopy. (C) Arrow depicts multilamellar body. Bar, 1 μm (A and B); bar, 100 nm (C); bar, 200 nm (D and E); bar, 100 nm (F).

ant of the HIV-1/IIIB strain of virus, HIV_{8x} is capable of productively infecting CD4-negative cells through CXCR4 coreceptor utilization (27). Both lymphoblast lines were infected to comparable levels, as determined by monitoring viral ERT products using real-time PCR (Fig. 2E) and intracellular Gag levels using flow cytometry (data not shown).

Virus production was quantified by two methods: the levels of RT activity in the supernatant measured over time and the extracellular levels of Gag measured as an indicator of virus release. By 11 days after infection, there was 10 times less RT activity present in the culture supernatant of the HIV_{8X}-infected NPCD lymphoblasts compared to the infected normal lymphoblasts (Fig. 2A). Proliferation rates for the infected NPCD cells were higher than those for the normal cells after infection (Fig. 2B). This could be a result of the limited spread of infection, as the infected NPCD cells exhibited markedly less cytopathic effect compared to the infected normal cells, which displayed classical hallmarks of HIV infection, such as syncytia formation and ballooning (data not shown).

Nonetheless, the decrease in RT activity in the NPCD cells became even more apparent when normalized by cell number. Four days after infection, RT activity detected in the culture supernatant from the infected NPCD cells was five times less than that measured from the infected normal cells upon normalization. An analysis of the amount of Gag present in the supernatant from infected cells revealed that by 30 days after infection there was a greater than 90% decrease in virus released from the NPCD lymphoblasts compared to the normal lymphoblasts (Fig. 2C).

To investigate the reasons why virus production in the NPCD lymphoblasts was limited, we tested the ability of progeny virions released from the HIV_{8X}-infected NPCD cells to infect susceptible cells. To achieve this, normal and NPCD lymphoblasts were infected with HIV_{8X} and after 15 days, virus-containing supernatants were collected and purified through a sucrose gradient. The purified virus was then used to infect Jurkat cells, and extracellular Gag levels were quantified as a measure of virus release over multiple rounds of infection. Even at the highest input, little or no virus was released from the Jurkat cells infected with progeny from the HIV_{8X}-infected NPCD lymphoblasts. In contrast, high levels of virus were readily detected upon infection of Jurkat cells with progeny from the infected normal lymphoblasts (Fig. 2D). Collectively, these findings demonstrate that loss of NPC1 function in lymphoblasts results in impaired release of viral particles upon HIV-1 infection. Furthermore, the relatively few viral particles released from NPC1-deficient cells are poorly infectious.

NPCD cells exhibit few HIV-1 budding events. The low virus yield from the HIV-1-infected NPCD lymphoblasts combined with their poor infectivity suggested that the virus was not undergoing proper assembly in those cells. To examine this further, normal and NPCD lymphoblasts were infected with HIV_{8X}, and at 20 days after infection the cells were analyzed by transmission electron microscopy (Fig. 3). As controls, noninfected normal and noninfected NPCD lymphoblasts were also examined. As expected, the noninfected NPCD cells exhibited classical hallmarks of NPC disease, including accumulation of multilamellar bodies and an abundance of L structures (Fig. 3B and C), neither of which were observed with the normal cells (Fig. 3A). Upon infection, both immature and mature viral particle budding events were observed at the plasma membrane in the normal lymphoblasts (Fig. 3D). In contrast, we did not observe progeny virions budding with normal morphology from the infected NPCD lymphoblasts, neither at the plasma membrane nor intracellularly (Fig. 3E and F).

The infected NPCD cells exhibited large vacuoles which showed no discernible budding events. This finding clearly demonstrates abnormal HIV-1 assembly in the absence of NPC1 function in lymphoblasts and may explain the poor infectivity of the viral particles released from these cells.

Inhibition of HIV-1 production in NPC1-deficient cells after a single cycle of infection or transfection is accompanied by normal levels of intracellular HIV-1 Gag. To further investigate the effects of the NPC1 mutation on HIV-1 replication, we

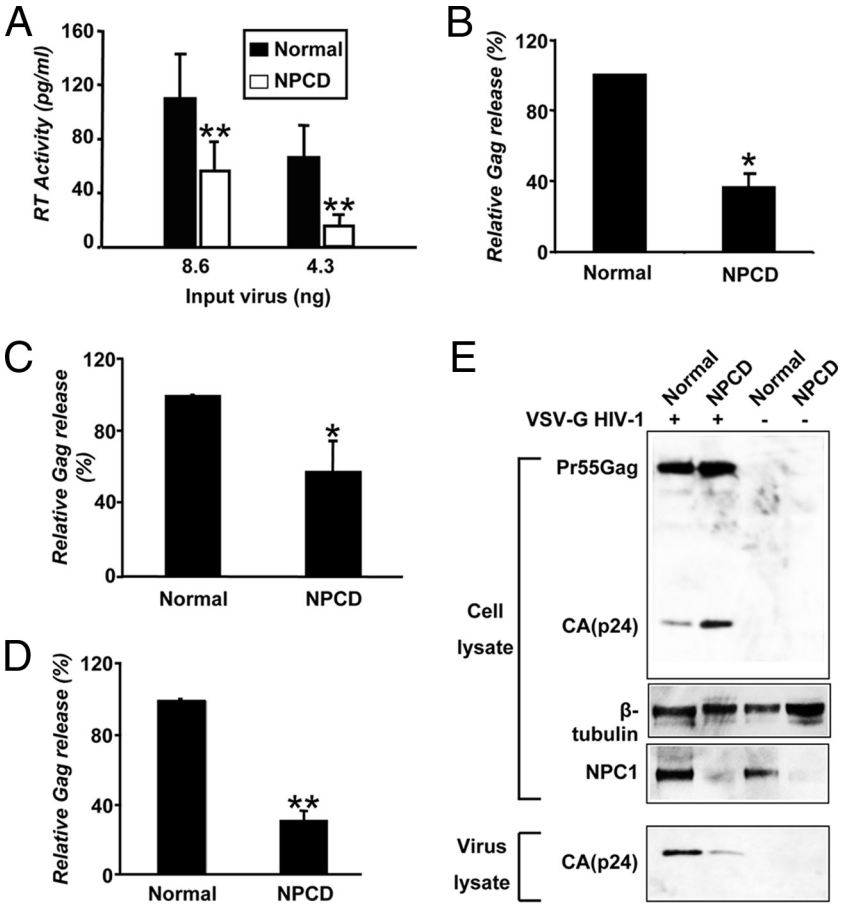

FIG. 4. Dominant inhibition of particle assembly/release in NPCD cells either infected with VSV-G-pseudotyped virus or transfected with a proviral clone and Gag expression vector. (A) The effects of NPCD lymphoblasts on NL4.3 viral particle release with VSV-G-pseudotyped virus infection. Normal (black bars) and NPCD B-lymphoblast (white bars) cells were infected with indicated concentrations of VSV-G HIV-1. RT activity in the supernatant was quantified after 48 h. (B) Normal and NPCD fibroblasts were infected with VSV-G HIV-1 (2 to 3 μg p24/10^6 cells). Gag antigen release into the supernatant was also measured by an antigen-capture ELISA. The relative amounts of Gag are percentages of infected normal cells (arbitrarily set as 100%). (C) Normal and NPCD fibroblasts were transfected with pNL4.3. 48 h posttransfection, the amount of Gag released into the supernatant was measured by a standard p24 ELISA. The relative amounts of Gag are percentages of transfected normal cells (arbitrarily set as 100%). The results shown represent the mean ± standard deviation from three independent experiments. *, $P < 0.005$, compared to infected normal fibroblasts. (D) NPCD and normal fibroblasts were transfected with a Gag expression vector. 48 h posttransfection, the amount of Gag released into the supernatant was measured by a standard p24 ELISA. Viral release data shown are normalized to percentages of infected/transfected cells, as determined by flow cytometry using anti-Gag antibody. The relative amounts of Gag are percentages of transfected normal cells (arbitrarily set as 100%). (E) Cells infected as described for panel B. After 96 h of infection, whole-cell lysates (upper three panels) and viral lysates (lower panel) were harvested and analyzed by immunoblotting using anti-Gag, anti-NPC1, and anti-β-tubulin antibodies. Data shown represent the mean ± standard deviations from three independent experiments. *, $P < 0.05$ **, $P < 0.001$, compared to normal cells (A, B, C, and D).

utilized a single-cycle HIV-1 virus pNL4.3 bearing the VSV-G protein on its surface to facilitate efficient infection. Normal and NPCD lymphoblasts were infected with VSV-G HIV-1. RT activity in the supernatant of the infected cell cultures was quantified 48 h later, as a measure of the level of infection. Upon normalization of cell number, compared to the normal lymphoblasts infected with VSV-G HIV-1, there was an approximately 50% decrease in RT activity in the NPCD lymphoblasts infected with the same virus (Fig. 4A).

NPCD fibroblasts were obtained from the same patient as the lymphoblasts, and when infected with VSV-G HIV-1, similar findings were observed. Using the standard p24 ELISA to quantify levels of Gag protein in supernatants from cells infected for 96 h, we observed a 60% reduction in the amount of virus released from the infected NPCD fibroblasts compared with normal fibroblasts (Fig. 4B). These results were confirmed when the NPCD fibroblasts were transfected with the pNL4.3 proviral clone, resulting in a 40 to 50% decrease in virus release compared to infected normal cells (Fig. 4C). Additionally, transfecting the NPCD fibroblasts with a Gag expression plasmid resulted in a 70% decrease in Gag release compared to normal cells (Fig. 4D).

Next, we performed a comparative analysis of viral protein production in VSV-G HIV-1-infected normal and NPCD fibroblasts. Infected cell lysates from the two infected cell types were analyzed by immunoblotting for the production of the structural viral protein Gag. Despite the readily apparent difference in the amounts of virus released from these cells, the

NPCD fibroblasts had comparable or slightly elevated levels of cell-associated Gag compared to infected normal cells. There was, however, a significant decrease in virus-associated Gag levels in the infected NPCD fibroblasts compared to the normal cells (Fig. 4E). These data confirm an important role for NPC1 in HIV-1 replication and indicate that the defect in virus replication in the NPCD cells is likely occurring during a late-assembly/release step of the replication cycle.

HIV-1 Gag protein accumulates in LE/L compartments in NPCD cells. Dysfunction in NPC1 protein results in altered intracellular trafficking of host proteins. Proteins that usually cycle from the LEs to the plasma membrane, such as MPR/IGF2, are mistargeted to the LE/L compartment in NPCD cells. Our findings indicate that while viral protein expression levels are normal in the NPCD cells, there is a significant reduction in virus production compared to normal cells. A reasonable explanation for this could be that in the NPCD cells, the viral proteins are trafficking abnormally, as is the case for some cellular proteins.

To determine if there were gross changes to Gag distribution in the absence of NPC1 activity, the localization of Gag was evaluated in normal and NPCD fibroblasts infected with VSV-G HIV-1. At 4 days after infection, the localization of both the Gag protein and either the LE marker CD63 or the L marker LAMP-2 was determined by double-label immunofluorescence, as shown in Fig. 5. In the normal fibroblasts, Gag was primarily diffuse, with some areas of well-organized foci evenly distributed throughout the cell. In these same cells, CD63 was concentrated in discrete puncta in perinuclear regions (Fig. 5A), while LAMP-2 puncta were found throughout the body of the cell (Fig. 5B). In the infected normal fibroblasts there was little or moderate colocalization between Gag and these two cellular proteins that mark the LE/L compartments.

In striking contrast, however, the infected NPCD fibroblasts exhibited a distinct localization of Gag, such that it was much more highly concentrated in the perinuclear area than was that observed with the normal cells. Furthermore, there was strong colocalization between Gag and CD63 proteins, as well as between Gag and LAMP-2 (Fig. 5A and B). The change in the distribution of these two cellular proteins is not surprising, as they both have been found in abundance in membranes of the multilamellar bodies characteristic of NPCD cells (Fig. 3C).

Similar results were also observed when cells were stained with the L dye LysoTracker Red, a weak base that accumulates in acidic compartments. There was strong colocalization between Gag and L compartments in the NPCD cells, while no colocalization was seen with the normal cells (Fig. 5C). Staining the infected NPCD cells with filipin showed Gag accumulating in the same subcellular compartment as the cholesterol (Fig. 5D). Quantitative analysis performed on the intracellular punctate distribution pattern of Gag revealed that CD63 puncta, total intracellular Gag, and Gag-to-CD63 colocalization were significantly increased in VSV-G HIV-1-infected NPCD cells compared to infected normal cells ($P < 0.001$) (Fig. 5E).

There was a strong correlation between total intracellular Gag and Gag colocalized with CD63 in the infected NPCD cells that was not found with infected normal cells ($R^2 = 0.7542$ versus $R^2 = 0.3942$, respectively) (Fig. 5F and G). Taken together, these findings indicate that in the absence of NPC1 function and as a result of the subsequent disruption of intracellular cholesterol trafficking pathways, HIV-1 Gag protein accumulates in LE/L compartments, which may account for the viral production impairment.

Normal HIV-1 biogenesis is restored in NPCD cells upon expression of a functional NPC1 protein, and overexpression of NPC1 increases HIV-1 release. In order to confirm that the NPC1 protein was directly responsible for the effect on HIV-1 replication observed with NPCD cells, we transfected these cells with an NPC1 cDNA vector to restore expression of the protein. Immunoblotting analysis confirmed increased expression of NPC1 after transfection of the NPCD cells. In both the normal and NPCD cells, the NPC1 expression levels increased proportionally from baseline as a consequence of transfection with the HIV-1 proviral clone pNL4.3 compared to nontransfected control cells (Fig. 6A, middle). This is unsurprising, as HIV-1 Nef induces multiple genes involved in cholesterol synthesis and homeostasis (51, 80, 88), and it is possible that it may induce NPC1 expression as well. Comparable levels of cell-associated Gag were observed with the HIV-1-expressing normal and NPCD cells, both in the presence and absence of exogenous NPC1 (Fig. 6A, top). However, virus-associated Gag was still greatly reduced in the NPCD cells (Fig. 6B). When the NPCD cells transfected with NPC1 were tested for their ability to support HIV-1 replication, they were found to release HIV-1 at levels similar to that of control cells (Fig. 6B).

Overexpression of NPC1 has been shown to increase the delivery of cholesterol from endosomal membranes to the plasma membrane (49). We have demonstrated that upon impairment of NPC1 function, despite similar Gag production, Gag release is drastically reduced. If NPC1 regulates the LE transport of Gag, overexpression of NPC1 should increase Gag release. To test this, we expressed NPC1 cDNA along with either a Gag expression plasmid or an HIV-1 full-length lentiviral expression plasmid (pNL4.3). TZM-bl cells were cotransfected with the Gag expression plasmid at a constant concentration and increasing amounts of the NPC1 plasmid. A dose-dependent enhancement of Gag released into the supernatant was detected that correlated with increased levels of NPC1 (Fig. 6C). Moreover, cotransfecting cells with the pNL4-3 and NPC1 plasmids resulted in a threefold increase in particle release relative to pEGFP control-transfected cells (Fig. 6D). Similar results were also observed when 293T cells were used to perform these experiments (data not shown). Taken together, these data confirm that lack of functional NPC1 expression in NPCD cells was responsible for both the NPC1 disease phenotype and restricted HIV-1 release in these cells.

Exposure of cells to 2-hydoxypropyl-β-cyclodextrin (2OHpβCD) effectively induces cellular cholesterol efflux. Recently, a study of a mouse model of NPCD showed that suggested 2OHpβCD treatments partially reverse the Niemann-Pick disease phenotype (43). Depletion of cholesterol from normal cells with 2OHpβCD did not alter viral production over time (data not shown); in contrast, treatment of NPCD cells with 2OHpβCD caused a dramatic increase in the level of virus release during 1-h exposure to the compound, and viral release declined to levels similar to those of untreated control cells at 2 h and 24 h posttreatment, presumably due to the metabolic turnover of cholesterol. These results suggest that HIV-1 assembly/release

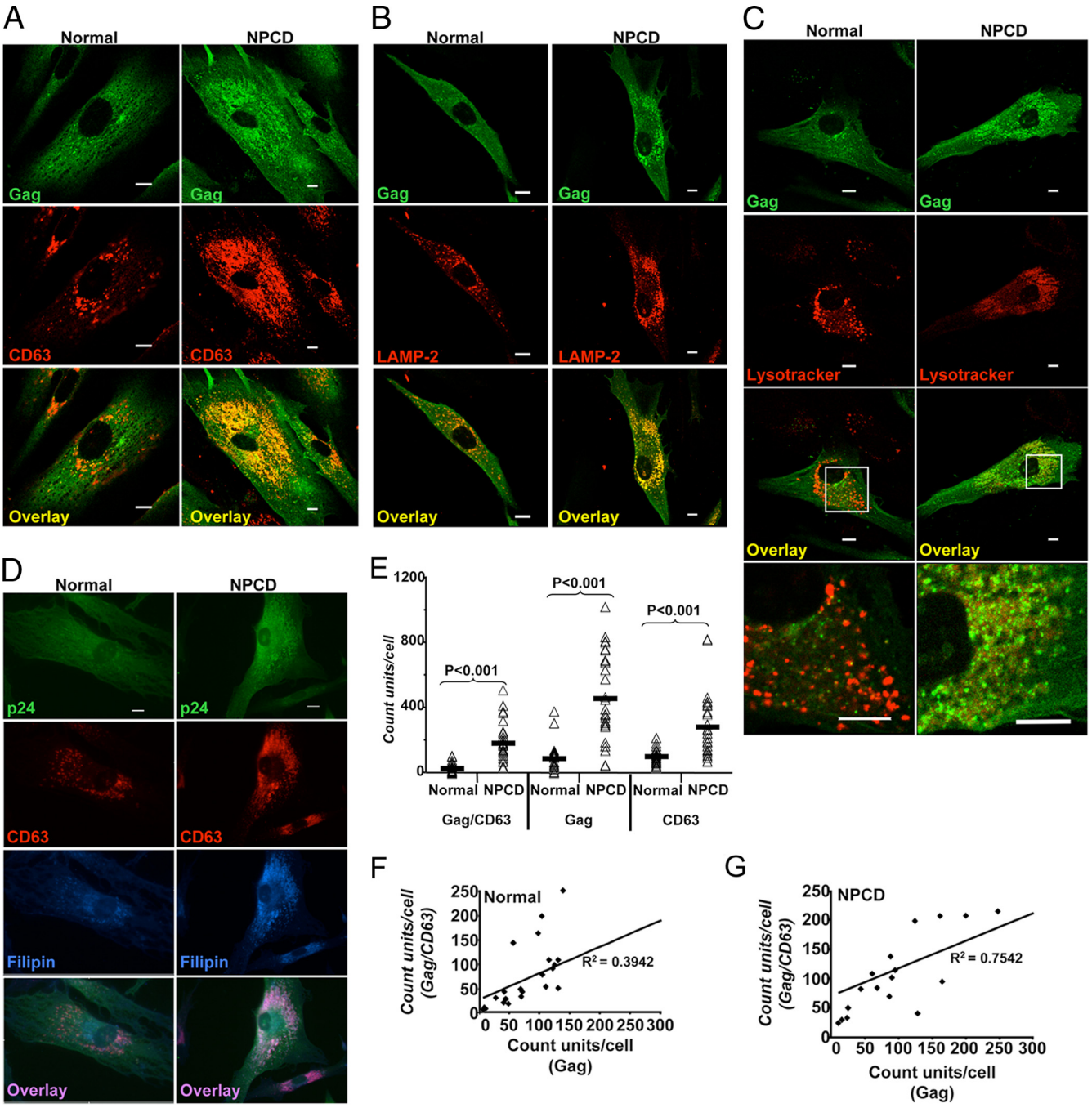

FIG. 5. Colocalization of HIV Gag and LE and L markers in NPCD fibroblasts cells. Primary NPCD and normal fibroblasts were infected with NL4.3-VSV-G-pseudotyped virus. Cells were fixed at 96 h postinfection and immunostained. (A, B, C and D) Gag is shown in green, the LE/L marker in red, cholesterol in blue, and colocalized pixels in yellow or pink. Size bars represent 10 μm. Gag (green) is seen colocalized extensively with LE/L marker (red) CD63 (A), Lamp2 (B), and Lysotracker Red (C) in NPCD cells. (D) Gag (green) is seen colocalized with cholesterol (blue) and CD63 (red) in NPCD cells. Cholesterol was stained with filipin. (E) Quantitation of Gag/CD63 colocalization. The intracellular puncta of Gag, CD63, and Gag colocalizing with CD63 were quantified using Nikon Elements Advanced Research software for 26 NPCD cells and normal cells each. Δ represents the puncta count from each cell, and — represents the mean of 26 cells in each group. Correlations between total intracellular Gag puncta and Gag puncta colocalizing with CD63 in normal cells (F) and NPCD cells (G).

could be rescued by induced cholesterol efflux. Overexpression of Rab9 in NPCD cells was shown to promote cholesterol and glycosphingolipid clearance (8, 84). However, we observed only a slight increase of virus release with Rab9 overexpression in NPCD cells either infected with VSV G-pseudotyped HIV-1 virus (data not shown) or cotransfected with a proviral clone (data not shown). Confocal microscopy revealed that overexpression of Rab9 in NPCD cells showed the same Gag phenotype as that of control NPCD cells (data now shown). The level of Rab9 expression and viral infection in these cells was deter-

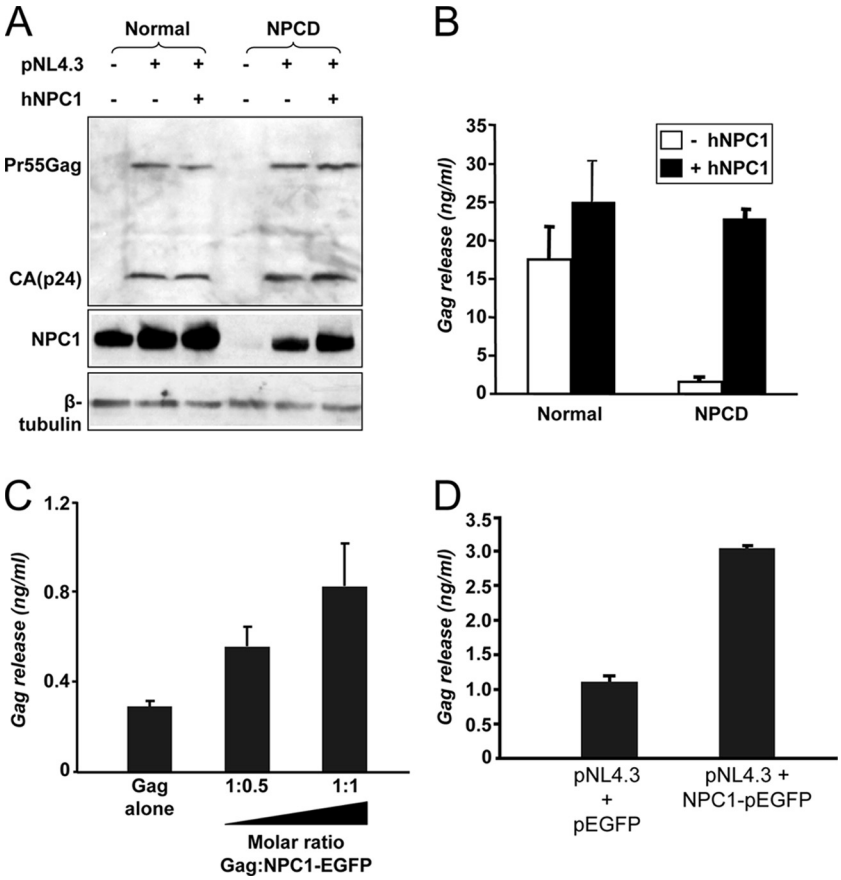

FIG. 6. Exogenous NPC1 restores Gag release in NPCD cells to normal levels, and NPC1 overexpression correlates with increased Gag release. (A, B) Normal or NPCD fibroblasts were cotransfected with the pNL4.3 proviral clone and either an NPC1 expression vector or empty vector. Samples were harvested after 24 h of transfection. (A) Cell lysates were collected and analyzed by immunoblotting with anti-NPC1 antibody after normalizing by amount of protein (top blot). The level of Gag protein and β-tubulin was detected by Western blotting with anti-Gag (middle) and anti-β-tubulin (bottom). (B) Amount of Gag released in the supernatant was quantified by a p24 ELISA. Data shown represent the mean ± standard deviation from two independent experiments. (C) Overexpression of NPC1 in TZM-bl cells increases Gag particle release. TZM-bl cells were transfected with a Gag plasmid and with increasing amounts of NPC1-enhanced GFP DNA, as indicated. Gag released in the supernatant was quantified by p24 capture ELISA. Data shown represent the mean±SD from two independent experiments. (D) Overexpression of NPC1 in TZM-bl cells increases viral particle release. TZM-bl cells were transfected with pNL4.3 proviral DNA and cotransfected with either pEGFP or NPC1-enhanced GFP. The amount of Gag released in the supernatant was quantified 48 h post transfection using p24 ELISA. Data shown represent the mean ±SD from two independent experiments.

mined by flow cytometry analysis (data not shown). These data indicate that Rab9 overexpression does not rescue Gag release in NPCD cells.

DISCUSSION

In this study we observed inhibition of HIV-1 replication in NPCD cells and in normal cells with the U18666A-induced NPCD phenotype. Overexpression of NPC1 in TZM-bl cells enhances HIV-1 release. The role of NPC1 in mediating viral protein trafficking is suggested by the observation of HIV-1 Gag accumulation in LE/L compartments in NPCD cells. NPC1 plays a major role in endocytic transport (35), L cholesterol efflux (42), and fatty acid efflux (9). Given HIV's need of the LE as a major site for protein sorting, virus assembly, budding, and acquisition of cholesterol critical for HIV assembly and infectivity (40, 41), these observations all support a role for NPC1 in HIV replication.

The NPC1 protein plays a pivotal role in both lipid sorting and vesicular trafficking (9, 35, 42). While NPC1 has been shown to work in a cooperative manner with NPC2 to traffic cholesterol within LE/L compartments (32), there is strong evidence that NPC1 also has a role in vesicular trafficking (29, 56). Live cell imaging studies of normal cells revealed NPC1 emerging from LE/Ls and undergoing rapid vectorial movement toward and away from both the nucleus and plasma membrane (35, 87). Such findings are consistent with the known role of NPC1 in mediating cargo transfer to the ER and plasma membrane (55, 85). In NPCD cells or U18666A-treated cells, the NPC1-mediated vesicular trafficking pathway seems to be paralyzed, as visualized by live cell imaging; in these cells the high-speed NPC1-containing organelles are largely absent (35, 87).

HIV-1 Gag is synthesized in the cytoplasm and then delivered to LEs by AP-3 (12). In some cells, such as macrophages, AP-3-mediated trafficking of Gag to the multivesicular bodies

(MVB) appears to be followed by viral budding into the lumen of the MVB. The intact viral particles within the MVB or "viral exosomes" may be transported subsequently to the cell surface for release. However, viruses seen in these internal structures may also be the result of particles bound by tetherin and internalized (54, 82). In most cell types, Gag further moves from the LEs to the plasma membrane to initiate budding. Although some host proteins, like the LE-to-TGN-associated protein Rab9 and the TGN-associated protein hPOSH, have been shown to be involved in the regulation of the late stages of Gag trafficking (1, 53), the detailed molecular mechanisms underlying this process are still not well characterized.

Here we revealed that the HIV-1 structural protein Gag accumulates in CD63- and Lamp-2-positive compartments and overlaps with the accumulated cholesterol in HIV-1-infected NPCD fibroblasts (Fig. 5). This result implies that Gag failed to export from the LE/L compartment and suggests that NPC1-mediated trafficking is critical for trafficking Gag from the LE to the plasma membrane.

Observations from various groups indicate that Gag strongly colocalizes with CD63 (57, 59, 81). It is possible that Gag and CD63 traffic together via the LE vesicular pathway. In NPCD cells, we observed that in addition to Gag, CD63 efflux from endosomes was also blocked, as demonstrated by decreased levels of the protein in the plasma membrane and increased intracellular CD63 levels (Fig. 5E) (as well as measured by flow cytometry [data not shown]). Impairment of NPC1 function further increases the colocalization between CD63 and Gag, as shown in Fig. 5A. This suggests that defects in NPC1-mediated trafficking results in sequestration of CD63 and Gag in the LE and implies that these two proteins traffic together via an LE vesicular pathway for endosome export.

These data also explain the previously recognized high degree of colocalization of these two molecules in normal cells. Both Gag and CD63 have been shown to transport to LEs via an AP-3-mediated mechanism (12, 68). Moreover, proper targeting of NPC1 is dependent on AP-3 (2), and Gag has been shown to interact with the AP-3 δ subunit via its MA domain. It is highly likely that NPC1 binds to AP-3 directly, and it is also possible that NPC1 and Gag directly interact. It appears that both NPC1 and CD63 share the same transport routes to the LE/L compartments as Gag.

An alternative, nonmutually exclusive model accounting for the role of NPC1 in Gag trafficking and HIV-1 release comes from observations of Rab9 in NPC1-mediated protein trafficking and in HIV-1 replication. Rabs are small GTPases involved in vesicular trafficking through the tethering of donor vesicles to target membrane (46). Rab9 mediates LE-to-TGN trafficking. Transport of mannose 6-phospate receptors from LEs to the TG is coordinated by Rab9 (44, 65) and requires the Rab9 effectors TIP47 and p40 (5, 10, 11). Kobayashi et al. have produced evidence that impaired Rab9 function is responsible for mannose 6-phospate receptor mistrafficking in NPCD cells (36). Further observations indicate prenylated Rab9 is trapped on LE membranes due to cholesterol accumulation, thereby inhibiting its function (18). Notably, Rab9 and TIP47 as well as other effectors that mediate LE-to-TG transport are required for HIV-1 replication (53). Reducing expression of Rab9 or its effector proteins with small interfering RNA dramatically decreases HIV-1 replication. HIV-1 Gag also accumulates in CD63-positive LE compartments in cells, wherein Rab9 expression has been suppressed using small interfering RNA (53). The dysfunction of Rab9 in NPCD cells could, at least in part, explain our observation of viral HIV assembly/release defects and Gag accumulation in LE/L compartments.

These observations raise the question as to whether sequestration of Gag in the LEs of NPCD cells is simply a result of Rab9 dysfunction, or whether NPC1 and Rab9 both have a direct role in mediating Gag and cholesterol transport. Our current studies show that the Gag accumulation patterns observed in the NPCD cells are different from that seen with the Rab9-deleted cells (53). In our studies, Gag was found not only to overlap with CD63 but also overlapped with L markers and accumulated cholesterol (Fig. 5B to D). This was not the case with Rab9-deleted cells. Thus, a defect in Rab9 function does not likely explain the impairment to Gag trafficking and viral production in NPCD cells. This suggestion is further supported by the fact that overexpression of Rab9 in NPCD cells, which has been shown to promote cholesterol and glycosphingolipid clearance from the NPCD LE/L compartments (8, 84), did not rescue the virus production or reverse Gag localization to LE/L compartments (data not shown).

Cholesterol, a major lipid component of the plasma membrane in eukaryotic cells, plays an essential role in maintaining membrane fluidity and architecture. Within the plasma membrane, cholesterol can segregate with sphingolipids and selective proteins to form distinct lipid raft complexes that act as ordered platforms for specific biological functions (71). HIV-1 also has been shown to use lipid rafts for budding and release (40, 41, 58). Cells tightly control the ratio of cholesterol and phospholipids in membranes, and this control is essential for maintaining function of specific proteins. NPC1 protein plays a pivotal role in endocytic vesicular traffic by regulating movement of lipids and other cargo. In addition to being a cargo of the pathway, cholesterol itself appears to modulate NPC1 vesicle-mediated transport from LE/Ls.

The activities of many integral membrane proteins are modulated by the physical properties of the membrane in which they reside, an example of which is Rab9. It may be that the sterol-sensing domain of NPC1 enables it to sense cellular lipid levels and that it functions to maintain a basal concentration of cholesterol in endosomal membranes. NPC1 may also affect the concentration and distribution of other cargo, as determined by cellular needs and endosomal vesicle mobility. Other NPC1 functional defects or increased NPC1 expression could disrupt lipid organization and lipid raft structure in both the plasma membrane and LE membranes (30, 45, 49) and thereby affect budding and release of HIV-1 particles.

In NPCD cells, LE membranes accumulate, resulting in the formation of aberrant compartments containing lipid lamellae bearing both LE and L markers (45, 52). The cholesterol level in the plasma membrane and the lipid raft content of the plasma membrane also increase (48, 77). Our data indicate that HIV-1 particle release is adversely affected as a result of the late endocytic organelle trafficking dysfunction found in U18666A-treated cells and in NPCD cells (Fig. 1C and 2B). These findings reinforce the importance of membrane lipids and lipid raft structure as budding platforms for HIV-1. The lack of infectivity of the few HIV-1 particles released by these

cells (Fig. 2D) could result from a virus envelope with altered lipid or protein composition.

To show if the virus production defect observed with NPCD cells is directly caused by the cholesterol accumulation, cholesterol efflux was induced in infected NPCD cells with 2OHpβCD. HIV-1 production by the cells was increased substantially in the first hour of treatment release (data not shown). The data indicate that cholesterol trafficking between the internal membrane and the plasma membrane is an important factor in the HIV release defect in NPCD cells.

In summary, we have identified an important and as yet undescribed role of the NPC1 protein in HIV-1 infection. We have demonstrated that NPC1 mutant cells are poor hosts for HIV-1 infection. In these cells, the Gag protein appears to be trapped in LE/L structures, resulting in impaired virus release. Additionally, a direct relationship between NPC1 expression levels and virus release was demonstrated with normal cells. Further studies to fully understand the role of NPC1 in HIV assembly and release, especially in relation to AP-3 and Rab9, may provide important new insights into HIV biology.

ACKNOWLEDGMENTS

This work was supported by NIH grants to J.E.K.H. (NIAD R21AI062408 and NICHD R01HD040772) and by NIH facilities grants U54NS041071-06, G12RR03032-19, U54CA91408, and U54RR019192-04.

We thank J. Hoxie for kindly providing a CD4-independent strain of HIV, M. P. Scott for provision of the NPC1-enhanced GFP plasmid, B. D. Liu for the pHEF VSV G plasmid, Suzanne Pfeffer for the Rab9 plasmid, Alvin George for ELISA experiment assistance, Waldemar Popik and Atanu Khatua for their technical assistance, and Jared Elzey for editorial assistance.

We declare that no competing interests exist.

REFERENCES

1. **Alroy, I., S. Tuvia, T. Greener, D. Gordon, H. M. Barr, D. Taglicht, R. Mandil-Levin, D. Ben-Avraham, D. Konforty, A. Nir, O. Levius, V. Bicoviski, M. Dori, S. Cohen, L. Yaar, O. Erez, O. Propheta-Meiran, M. Koskas, E. Caspi-Bachar, I. Alchanati, A. Sela-Brown, H. Moskowitz, U. Tessmer, U. Schubert, and Y. Reiss.** 2005. The trans-Golgi network-associated human ubiquitin-protein ligase POSH is essential for HIV type 1 production. Proc. Natl. Acad. Sci. USA **102:**1478–1483.
2. **Berger, A. C., G. Salazar, M. L. Styers, K. A. Newell-Litwa, E. Werner, R. A. Maue, A. H. Corbett, and V. Faundez.** 2007. The subcellular localization of the Niemann-Pick Type C proteins depends on the adaptor complex AP-3. J. Cell Sci. **120:**3640–3652.
3. **Bishop, N. E.** 2003. Dynamics of endosomal sorting. Int. Rev. Cytol. **232:**1–57.
4. **Campbell, S. M., S. M. Crowe, and J. Mak.** 2001. Lipid rafts and HIV-1: from viral entry to assembly of progeny virions. J. Clin. Virol. **22:**217–227.
5. **Carroll, K. S., J. Hanna, I. Simon, J. Krise, P. Barbero, and S. R. Pfeffer.** 2001. Role of Rab9 GTPase in facilitating receptor recruitment by TIP47. Science **292:**1373–1376.
6. **Cenedella, R. J., and G. G. Bierkamper.** 1979. Mechanism of cataract production by 3-beta(2-diethylaminoethoxy) androst-5-en-17-one hydrochloride, U18666A: an inhibitor of cholesterol biosynthesis. Exp. Eye Res. **28:** 673–688.
7. **Chertova, E., O. Chertov, L. V. Coren, J. D. Roser, C. M. Trubey, J. W. Bess, Jr., R. C. Sowder II, E. Barsov, B. L. Hood, R. J. Fisher, K. Nagashima, T. P. Conrads, T. D. Veenstra, J. D. Lifson, and D. E. Ott.** 2006. Proteomic and biochemical analysis of purified human immunodeficiency virus type 1 produced from infected monocyte-derived macrophages. J. Virol. **80:**9039–9052.
8. **Choudhury, A., M. Dominguez, V. Puri, D. K. Sharma, K. Narita, C. L. Wheatley, D. L. Marks, and R. E. Pagano.** 2002. Rab proteins mediate Golgi transport of caveola-internalized glycosphingolipids and correct lipid trafficking in Niemann-Pick C cells. J. Clin. Investig. **109:**1541–1550.
9. **Davies, J. P., F. W. Chen, and Y. A. Ioannou.** 2000. Transmembrane molecular pump activity of Niemann-Pick C1 protein. Science **290:**2295–2298.
10. **Diaz, E., and S. R. Pfeffer.** 1998. TIP47: a cargo selection device for mannose 6-phosphate receptor trafficking. Cell **93:**433–443.
11. **Diaz, E., F. Schimmoller, and S. R. Pfeffer.** 1997. A novel Rab9 effector required for endosome-to-TGN transport. J. Cell Biol. **138:**283–290.
12. **Dong, X., H. Li, A. Derdowski, L. Ding, A. Burnett, X. Chen, T. R. Peters, T. S. Dermody, E. Woodruff, J. J. Wang, and P. Spearman.** 2005. AP-3 directs the intracellular trafficking of HIV-1 Gag and plays a key role in particle assembly. Cell **120:**663–674.
13. **Duriatti, A., P. Bouvier-Nave, P. Benveniste, F. Schuber, L. Delprino, G. Balliano, and L. Cattel.** 1985. In vitro inhibition of animal and higher plants 2,3-oxidosqualene-sterol cyclases by 2-aza-2,3-dihydrosqualene and derivatives, and by other ammonium-containing molecules. Biochem. Pharmacol. **34:**2765–2777.
14. **Fader, C. M., and M. I. Colombo.** 2009. Autophagy and multivesicular bodies: two closely related partners. Cell Death Differ. **16:**70–78.
15. **Falguieres, T., P. P. Luyet, and J. Gruenberg.** 2008. Molecular assemblies and membrane domains in multivesicular endosome dynamics. Exp. Cell Res. [Epub ahead of print.] doi:10.1016/j.yexcr.2008.12.006.
16. **Finzi, A., A. Brunet, Y. Xiao, J. Thibodeau, and E. A. Cohen.** 2006. Major histocompatibility complex class II molecules promote human immunodeficiency virus type 1 assembly and budding to late endosomal/multivesicular body compartments. J. Virol. **80:**9789–9797.
17. **Frolov, A., S. E. Zielinski, J. R. Crowley, N. Dudley-Rucker, J. E. Schaffer, and D. S. Ory.** 2003. NPC1 and NPC2 regulate cellular cholesterol homeostasis through generation of low density lipoprotein cholesterol-derived oxysterols. J. Biol. Chem. **278:**25517–25525.
18. **Ganley, I. G., and S. R. Pfeffer.** 2006. Cholesterol accumulation sequesters Rab9 and disrupts late endosome function in NPC1-deficient cells. J. Biol. Chem. **281:**17890–17899.
19. **Garver, W. S., and R. A. Heidenreich.** 2002. The Niemann-Pick C proteins and trafficking of cholesterol through the late endosomal/lysosomal system. Curr. Mol. Med. **2:**485–505.
20. **Gelsthorpe, M. E., N. Baumann, E. Millard, S. E. Gale, S. J. Langmade, J. E. Schaffer, and D. S. Ory.** 2008. Niemann-Pick type C1 I1061T mutant encodes a functional protein that is selected for endoplasmic reticulum-associated degradation due to protein misfolding. J. Biol. Chem. **283:**8229–8236.
21. **Gong, Y., M. Duvvuri, M. B. Duncan, J. Liu, and J. P. Krise.** 2006. Niemann-Pick C1 protein facilitates the efflux of the anticancer drug daunorubicin from cells according to a novel vesicle-mediated pathway. J. Pharmacol. Exp. Ther. **316:**242–247.
22. **Gould, S. J., A. M. Booth, and J. E. Hildreth.** 2003. The Trojan exosome hypothesis. Proc. Natl. Acad. Sci. USA **100:**10592–10597.
23. **Graham, D. R., E. Chertova, J. M. Hilburn, L. O. Arthur, and J. E. Hildreth.** 2003. Cholesterol depletion of human immunodeficiency virus type 1 and simian immunodeficiency virus with beta-cyclodextrin inactivates and permeabilizes the virions: evidence for virion-associated lipid rafts. J. Virol. **77:**8237–8248.
24. **Grigorov, B., F. Arcanger, P. Roingeard, J. L. Darlix, and D. Muriaux.** 2006. Assembly of infectious HIV-1 in human epithelial and T-lymphoblastic cell lines. J. Mol. Biol. **359:**848–862.
25. **Guyader, M., E. Kiyokawa, L. Abrami, P. Turelli, and D. Trono.** 2002. Role for human immunodeficiency virus type 1 membrane cholesterol in viral internalization. J. Virol. **76:**10356–10364.
26. **Hendricks, L. C., M. McCaffery, G. E. Palade, and M. G. Farquhar.** 1993. Disruption of endoplasmic reticulum to Golgi transport leads to the accumulation of large aggregates containing beta-COP in pancreatic acinar cells. Mol. Biol. Cell **4:**413–424.
27. **Hoffman, T. L., C. C. LaBranche, W. Zhang, G. Canziani, J. Robinson, I. Chaiken, J. A. Hoxie, and R. W. Doms.** 1999. Stable exposure of the coreceptor-binding site in a CD4-independent HIV-1 envelope protein. Proc. Natl. Acad. Sci. USA **96:**6359–6364.
28. **Holtta-Vuori, M., and E. Ikonen.** 2006. Endosomal cholesterol traffic: vesicular and non-vesicular mechanisms meet. Biochem. Soc. Trans. **34:**392–394.
29. **Holtta-Vuori, M., J. Maatta, O. Ullrich, E. Kuismanesn, and E. Ikonen.** 2000. Mobilization of late-endosomal cholesterol is inhibited by Rab guanine nucleotide dissociation inhibitor. Curr. Biol. **10:**95–98.
30. **Incardona, J. P., and S. Eaton.** 2000. Cholesterol in signal transduction. Curr. Opin. Cell Biol. **12:**193–203.
31. **Infante, R. E., A. Radhakrishnan, L. Abi-Mosleh, L. N. Kinch, M. L. Wang, N. V. Grishin, J. L. Goldstein, and M. S. Brown.** 2008. Purified NPC1 protein. II. Localization of sterol binding to a 240-amino acid soluble luminal loop. J. Biol. Chem. **283:**1064–1075.
32. **Infante, R. E., M. L. Wang, A. Radhakrishnan, H. J. Kwon, M. S. Brown, and J. L. Goldstein.** 2008. NPC2 facilitates bidirectional transfer of cholesterol between NPC1 and lipid bilayers, a step in cholesterol egress from lysosomes. Proc. Natl. Acad. Sci. USA **105:**15287–15292.
33. **Kaufmann, A. M., and J. P. Krise.** 2008. Niemann-Pick C1 functions in regulating lysosomal amine content. J. Biol. Chem. **283:**24584–24593.
34. **Khatua, A. K., H. E. Taylor, J. E. Hildreth, and W. Popik.** 2009. Exosomes packaging APOBEC3G confer human immunodeficiency virus resistance to recipient cells. J. Virol. **83:**512–521.
35. **Ko, D. C., M. D. Gordon, J. Y. Jin, and M. P. Scott.** 2001. Dynamic movements of organelles containing Niemann-Pick C1 protein: NPC1 involvement in late endocytic events. Mol. Biol. Cell **12:**601–614.
36. **Kobayashi, T., M. H. Beuchat, M. Lindsay, S. Frias, R. D. Palmiter, H. Sakuraba, R. G. Parton, and J. Gruenberg.** 1999. Late endosomal mem-

branes rich in lysobisphosphatidic acid regulate cholesterol transport. Nat. Cell Biol. **1:**113–118.

37. **Levade, T., A. Maret, R. Salvayre, N. Livni, P. Rogalle, and L. Douste-Blazy.** 1986. Biochemical and ultrastructural studies on an Epstein-Barr virus-transformed lymphoid cell line from a Niemann-Pick disease type C patient. Biochim. Biophys. Acta **877:**415–422.
38. **Levade, T., R. Salvayre, G. Lenoir, and L. Douste-Blazy.** 1984. Sphingomyelinase and nonspecific phosphodiesterase activities in Epstein-Barr virus-transformed lymphoid cell lines from Niemann-Pick disease A, B and C. Biochim. Biophys. Acta **793:**321–324.
39. **Li, X. Y., F. Guo, L. Zhang, L. Kleiman, and S. Cen.** 2007. APOBEC3G inhibits DNA strand transfer during HIV-1 reverse transcription. J. Biol. Chem. **282:**32065–32074.
40. **Liao, Z., L. M. Cimakasky, R. Hampton, D. H. Nguyen, and J. E. Hildreth.** 2001. Lipid rafts and HIV pathogenesis: host membrane cholesterol is required for infection by HIV type 1. AIDS Res. Hum Retrovir. **17:**1009–1019.
41. **Liao, Z., D. R. Graham, and J. E. Hildreth.** 2003. Lipid rafts and HIV pathogenesis: virion-associated cholesterol is required for fusion and infection of susceptible cells. AIDS Res. Hum. Retrovir. **19:**675–687.
42. **Liscum, L.** 2000. Niemann-Pick type C mutations cause lipid traffic jam. Traffic **1:**218–225.
43. **Liu, B., S. D. Turley, D. K. Burns, A. M. Miller, J. J. Repa, and J. M. Dietschy.** 2009. Reversal of defective lysosomal transport in NPC disease ameliorates liver dysfunction and neurodegeneration in the *npc1*$^{-/-}$ mouse. Proc. Natl. Acad. Sci. USA **106:**2377–2382.
44. **Lombardi, D., T. Soldati, M. A. Riederer, Y. Goda, M. Zerial, and S. R. Pfeffer.** 1993. Rab9 functions in transport between late endosomes and the trans Golgi network. EMBO J. **12:**677–682.
45. **Lusa, S., T. S. Blom, E. L. Eskelinen, E. Kuismanen, J. E. Mansson, K. Simons, and E. Ikonen.** 2001. Depletion of rafts in late endocytic membranes is controlled by NPC1-dependent recycling of cholesterol to the plasma membrane. J. Cell Sci. **114:**1893–1900.
46. **Martinez, O., and B. Goud.** 1998. Rab proteins. Biochim. Biophys. Acta **1404:**101–112.
47. **Mayran, N., R. G. Parton, and J. Gruenberg.** 2003. Annexin II regulates multivesicular endosome biogenesis in the degradation pathway of animal cells. EMBO J. **22:**3242–3253.
48. **Miersch, S., M. G. Espey, R. Chaube, A. Akarca, R. Tweten, S. Ananvoranich, and B. Mutus.** 2008. Plasma membrane cholesterol content affects nitric oxide diffusion dynamics and signaling. J. Biol. Chem. **283:**18513–18521.
49. **Millard, E. E., K. Srivastava, L. M. Traub, J. E. Schaffer, and D. S. Ory.** 2000. Niemann-pick type C1 (NPC1) overexpression alters cellular cholesterol homeostasis. J. Biol. Chem. **275:**38445–38451.
50. **Morris, J. A., D. Zhang, K. G. Coleman, J. Nagle, P. G. Pentchev, and E. D. Carstea.** 1999. The genomic organization and polymorphism analysis of the human Niemann-Pick C1 gene. Biochem. Biophys. Res. Commun. **261:**493–498.
51. **Mujawar, Z., H. Rose, M. P. Morrow, T. Pushkarsky, L. Dubrovsky, N. Mukhamedova, Y. Fu, A. Dart, J. M. Orenstein, Y. V. Bobryshev, M. Bukrinsky, and D. Sviridov.** 2006. Human immunodeficiency virus impairs reverse cholesterol transport from macrophages. PLoS Biol. **4:**e365.
52. **Mukherjee, S., and F. R. Maxfield.** 2004. Lipid and cholesterol trafficking in NPC. Biochim. Biophys. Acta **1685:**28–37.
53. **Murray, J. L., M. Mavrakis, N. J. McDonald, M. Yilla, J. Sheng, W. J. Bellini, L. Zhao, J. M. Le Doux, M. W. Shaw, C. C. Luo, J. Lippincott-Schwartz, A. Sanchez, D. H. Rubin, and T. W. Hodge.** 2005. Rab9 GTPase is required for replication of human immunodeficiency virus type 1, filoviruses, and measles virus. J. Virol. **79:**11742–11751.
54. **Neil, S. J., T. Zang, and P. D. Bieniasz.** 2008. Tetherin inhibits retrovirus release and is antagonized by HIV-1 Vpu. Nature **451:**425–430.
55. **Neufeld, E. B., A. M. Cooney, J. Pitha, E. A. Dawidowicz, N. K. Dwyer, P. G. Pentchev, and E. J. Blanchette-Mackie.** 1996. Intracellular trafficking of cholesterol monitored with a cyclodextrin. J. Biol. Chem. **271:**21604–21613.
56. **Neufeld, E. B., M. Wastney, S. Patel, S. Suresh, A. M. Cooney, N. K. Dwyer, C. F. Roff, K. Ohno, J. A. Morris, E. D. Carstea, J. P. Incardona, J. F. Strauss III, M. T. Vanier, M. C. Patterson, R. O. Brady, P. G. Pentchev, and E. J. Blanchette-Mackie.** 1999. The Niemann-Pick C1 protein resides in a vesicular compartment linked to retrograde transport of multiple lysosomal cargo. J. Biol. Chem. **274:**9627–9635.
57. **Nguyen, D. G., A. Booth, S. J. Gould, and J. E. Hildreth.** 2003. Evidence that HIV budding in primary macrophages occurs through the exosome release pathway. J. Biol. Chem. **278:**52347–52354.
58. **Nguyen, D. H., and J. E. Hildreth.** 2000. Evidence for budding of human immunodeficiency virus type 1 selectively from glycolipid-enriched membrane lipid rafts. J. Virol. **74:**3264–3272.
59. **Nydegger, S., M. Foti, A. Derdowski, P. Spearman, and M. Thali.** 2003. HIV-1 egress is gated through late endosomal membranes. Traffic **4:**902–910.
60. **Patel, S. C., S. Suresh, U. Kumar, C. Y. Hu, A. Cooney, E. J. Blanchette-Mackie, E. B. Neufeld, R. C. Patel, R. O. Brady, Y. C. Patel, P. G. Pentchev, and W. Y. Ong.** 1999. Localization of Niemann-Pick C1 protein in astrocytes: implications for neuronal degeneration in Niemann-Pick type C disease. Proc. Natl. Acad. Sci. USA **96:**1657–1662.
61. **Pentchev, P. G., R. O. Brady, E. J. Blanchette-Mackie, M. T. Vanier, E. D. Carstea, C. C. Parker, E. Goldin, and C. F. Roff.** 1994. The Niemann-Pick C lesion and its relationship to the intracellular distribution and utilization of LDL cholesterol. Biochim. Biophys. Acta **1225:**235–243.
62. **Phillips, W. A., and J. Avigan.** 1963. Inhibition of cholesterol biosynthesis in the rat by 3 beta-(2-diethylaminoethoxy) androst5-en-17-one hydrochloride. Proc. Soc. Exp. Biol. Med. **112:**233–236.
63. **Piper, R. C., and D. J. Katzmann.** 2007. Biogenesis and function of multivesicular bodies. Annu. Rev. Cell Dev. Biol. **23:**519–547.
64. **Popik, W., T. M. Alce, and W. C. Au.** 2002. Human immunodeficiency virus type 1 uses lipid raft-colocalized CD4 and chemokine receptors for productive entry into CD4$^+$ T cells. J. Virol. **76:**4709–4722.
65. **Riederer, M. A., T. Soldati, A. D. Shapiro, J. Lin, and S. R. Pfeffer.** 1994. Lysosome biogenesis requires Rab9 function and receptor recycling from endosomes to the trans-Golgi network. J. Cell Biol. **125:**573–582.
66. **Roff, C. F., E. Goldin, M. E. Comly, A. Cooney, A. Brown, M. T. Vanier, S. P. Miller, R. O. Brady, and P. G. Pentchev.** 1991. Type C Niemann-Pick disease: use of hydrophobic amines to study defective cholesterol transport. Dev. Neurosci. **13:**315–319.
67. **Roos, J. W., M. F. Maughan, Z. Liao, J. E. Hildreth, and J. E. Clements.** 2000. LuSIV cells: a reporter cell line for the detection and quantitation of a single cycle of HIV and SIV replication. Virology **273:**307–315.
68. **Rous, B. A., B. J. Reaves, G. Ihrke, J. A. Briggs, S. R. Gray, D. J. Stephens, G. Banting, and J. P. Luzio.** 2002. Role of adaptor complex AP-3 in targeting wild-type and mutated CD63 to lysosomes. Mol. Biol. Cell **13:**1071–1082.
69. **Russell, M. R., D. P. Nickerson, and G. Odorizzi.** 2006. Molecular mechanisms of late endosome morphology, identity and sorting. Curr. Opin. Cell Biol. **18:**422–428.
70. **Sexton, R. C., S. R. Panini, F. Azran, and H. Rudney.** 1983. Effects of 3 beta-[2-(diethylamino)ethoxy]androst-5-en-17-one on the synthesis of cholesterol and ubiquinone in rat intestinal epithelial cell cultures. Biochemistry **22:**5687–5692.
71. **Simons, K., and E. Ikonen.** 1997. Functional rafts in cell membranes. Nature **387:**569–572.
72. **Steinberg, S. J., C. P. Ward, and A. H. Fensom.** 1994. Complementation studies in Niemann-Pick disease type C indicate the existence of a second group. J. Med. Genet. **31:**317–320.
73. **Sugii, S., P. C. Reid, N. Ohgami, H. Du, and T. Y. Chang.** 2003. Distinct endosomal compartments in early trafficking of low density lipoprotein-derived cholesterol. J. Biol. Chem. **278:**27180–27189.
74. **Tomiyama, Y., S. Waguri, S. Kanamori, S. Kametaka, M. Wakasugi, M. Shibata, S. Ebisu, and Y. Uchiyama.** 2004. Early-phase redistribution of the cation-independent mannose 6-phosphate receptor by U18666A treatment in HeLa cells. Cell Tissue Res. **317:**253–264.
75. **Tseng, T. T., K. S. Gratwick, J. Kollman, D. Park, D. H. Nies, A. Goffeau, and M. H. Saier, Jr.** 1999. The RND permease superfamily: an ancient, ubiquitous and diverse family that includes human disease and development proteins. J. Mol. Microbiol. Biotechnol. **1:**107–125.
76. **Urano, Y., H. Watanabe, S. R. Murphy, Y. Shibuya, Y. Geng, A. A. Peden, C. C. Chang, and T. Y. Chang.** 2008. Transport of LDL-derived cholesterol from the NPC1 compartment to the ER involves the trans-Golgi network and the SNARE protein complex. Proc. Natl. Acad. Sci. USA **105:**16513–16518.
77. **Vainio, S., I. Bykov, M. Hermansson, E. Jokitalo, P. Somerharju, and E. Ikonen.** 2005. Defective insulin receptor activation and altered lipid rafts in Niemann-Pick type C disease hepatocytes. Biochem. J. **391:**465–472.
78. **van der Goot, F. G., and J. Gruenberg.** 2006. Intra-endosomal membrane traffic. Trends Cell Biol. **16:**514–521.
79. **Vanier, M. T., S. Duthel, C. Rodriguez-Lafrasse, P. Pentchev, and E. D. Carstea.** 1996. Genetic heterogeneity in Niemann-Pick C disease: a study using somatic cell hybridization and linkage analysis. Am. J. Hum. Genet. **58:**118–125.
80. **van 't Wout, A. B., J. V. Swain, M. Schindler, U. Rao, M. S. Pathmajeyan, J. I. Mullins, and F. Kirchhoff.** 2005. Nef induces multiple genes involved in cholesterol synthesis and uptake in human immunodeficiency virus type 1-infected T cells. J. Virol. **79:**10053–10058.
81. **von Schwedler, U. K., M. Stuchell, B. Muller, D. M. Ward, H. Y. Chung, E. Morita, H. E. Wang, T. Davis, G. P. He, D. M. Cimbora, A. Scott, H. G. Krausslich, J. Kaplan, S. G. Morham, and W. I. Sundquist.** 2003. The protein network of HIV budding. Cell **114:**701–713.
82. **Waheed, A. A., S. D. Ablan, F. Soheilian, K. Nagashima, A. Ono, C. P. Schaffner, and E. O. Freed.** 2008. Inhibition of human immunodeficiency virus type 1 assembly and release by the cholesterol-binding compound amphotericin B methyl ester: evidence for Vpu dependence. J. Virol. **82:**9776–9781.
83. **Walter, M., F. W. Chen, F. Tamari, R. Wang, and Y. A. Ioannou.** 2009. Endosomal lipid accumulation in NPC1 leads to inhibition of PKC, hypophosphorylation of vimentin and Rab9 entrapment. Biol. Cell **101:**141–152.

84. **Walter, M., J. P. Davies, and Y. A. Ioannou.** 2003. Telomerase immortalization upregulates Rab9 expression and restores LDL cholesterol egress from Niemann-Pick C1 late endosomes. J. Lipid Res. **44:**243–253.
85. **Wojtanik, K. M., and L. Liscum.** 2003. The transport of low density lipoprotein-derived cholesterol to the plasma membrane is defective in NPC1 cells. J. Biol. Chem. **278:**14850–14856.
86. **Yamamoto, T., E. Nanba, H. Ninomiya, K. Higaki, M. Taniguchi, H. Zhang, S. Akaboshi, Y. Watanabe, T. Takeshima, K. Inui, S. Okada, A. Tanaka, N. Sakuragawa, G. Millat, M. T. Vanier, J. A. Morris, P. G. Pentchev, and K. Ohno.** 1999. NPC1 gene mutations in Japanese patients with Niemann-Pick disease type C. Hum. Genet. **105:**10–16.
87. **Zhang, M., N. K. Dwyer, D. C. Love, A. Cooney, M. Comly, E. Neufeld, P. G. Pentchev, E. J. Blanchette-Mackie, and J. A. Hanover.** 2001. Cessation of rapid late endosomal tubulovesicular trafficking in Niemann-Pick type C1 disease. Proc. Natl. Acad. Sci. USA **98:**4466–4471.
88. **Zheng, Y. H., A. Plemenitas, C. J. Fielding, and B. M. Peterlin.** 2003. Nef increases the synthesis of and transports cholesterol to lipid rafts and HIV-1 progeny virions. Proc. Natl. Acad. Sci. USA **100:**8460–8465.